DOING HYDROLOGY BACKWARD: ESTIMATING MOUNTAIN PRECIPITATION PATTERNS FROM STREAMFLOW

Brian Henn[1], Martyn P. Clark[2], Dmitri Kavetski[3], and Jessica D. Lundquist[4]

ABSTRACT

Estimation of basin-mean precipitation in mountainous areas may be difficult due to high spatial variability and time-varying precipitation patterns. Streamflow offers additional information about the water balance of the basin with which to estimate precipitation. We apply a methodology for inferring basin-mean precipitation from streamflow using Bayes' Theorem, and adapt this approach to snow-dominated basins in the Sierra Nevada mountain range of California. As part of this approach, we develop and couple a temperature-index snow model to an existing lumped hydrologic model. We infer 1981-2006 annual average precipitation across four basins and compare the results to those obtained from similar approaches based on climatological precipitation patterns. We also use the approach to identify an example of year-to-year variability in precipitation patterns, finding that the inferred precipitation patterns generally match other observations from two anomalous water years. The method offers the potential for inferring spatial precipitation patterns at a level of precision that could improve upon current methods. Future work on this approach will focus on identifying spatial patterns of precipitation across a more extensive collection of basins and water years. (KEYWORDS: precipitation, streamflow, water balance, Bayes)

INTRODUCTION

Estimating basin-mean precipitation in complex terrain is difficult due to uncertainty in both the precipitation gauges' horizontal and topographical representativeness relative to the basin (Milly and Dunne, 2002). Inadequate gauge spatial density or distribution with basin elevation can lead to errors on the order of 100% or greater in basin-mean precipitation. Both problems are particularly acute in mountain basins, compared to low-elevation basins, due to the greater spatial variability of orographic precipitation (Roe, 2005) and the lack meteorological stations at higher elevations (Daly et al., 2008; Lundquist et al., 2003; Luce et al., 2013; Adam et al., 2006). Additionally, mountain precipitation gauges may also contain biases of uncertain magnitude due to undercatch of snow and rain, as well as gauge icing (Rasmussen et al., 2011; Sieck et al., 2007). Manual access for wintertime gauge maintenance may be extremely difficult at mountain sites.

As a result of these factors, the observations available to estimate mountain basin-mean precipitation may be both spatially inadequate and of high uncertainty in many locations. The uncertainty in mountain precipitation hinders our ability to accurately predict rain-driven mountain basin floods, runoff volumes for water supply operations and summertime low flows from high-elevation snowmelt. Problems with gauge uncertainty and representativeness have also hindered attempts to compare hydrologic model structures and forcing datasets (Mizukami and Smith, 2012; Wayand et al., 2013). Similarly, the relatively poor knowledge of high-elevation spatial precipitation patterns limits our ability to validate and improve the simulation of precipitation in research and operational weather models (Jankov et al., 2009). Thus, constraining the uncertainty in spatially-distributed precipitation in mountain basins would improve many aspects of both hydrology and meteorology.

Streamflow is widely measured and has a well-understood link to basin-mean precipitation. From a mass balance perspective, streamflow must equal basin-mean precipitation minus evapotranspiration and changes in storage:

$$Q = \bar{P} - \overline{ET} - \Delta S \quad [1]$$

Paper presented Western Snow Conference 2014

[1] Brian Henn, Department of Civil and Environmental Engineering, University of Washington, Seattle, WA, bhenn@u.washington.edu

[2] Martyn P. Clark, National Center for Atmospheric Research, Boulder, CO, mclark@ucar.edu

[3] Dmitri Kavetski, School of Civil, Environmental and Mining Engineering, University of Adelaide, Adelaide, South Australia, dmitri.kavetski@gmail.com

[4] Jessica D. Lundquist, Department of Civil and Environmental Engineering, University of Washington, Seattle, WA, jdlund@u.washington.edu

where overbars indicate quantities averaged over the basin area. Thus, if Q is measured relatively accurately, and $\overline{ET}$ and ΔS can also be determined, then basin-mean precipitation can be inferred. This approach has been termed "doing hydrology backward" (Kirchner, 2009; Vrugt et al., 2008). In this study, we infer basin-mean precipitation in mountainous basins using streamflow records, with the goal of reducing the uncertainty in precipitation observations by employing the additional information about the basin hydrologic system that streamflow provides.

This approach employs gauge observations of precipitation somewhere in or near the basins of interest. However, we assume that due to spatial variability and gauge undercatch, the gauge record has an unknown bias relative to the "true" basin-mean precipitation. We define a precipitation multiplier which relates the gauge precipitation to the true precipitation. The multiplier is then calibrated during the process of fitting the modeled streamflow from a hydrologic model to observed streamflow. This approach has been applied previously to better understand errors in precipitation records (Kavetski et al., 2006; Vrugt et al., 2008).

Inferring Spatial Precipitation Patterns in the Sierra Nevada

We apply the approach of retrospectively estimating basin-mean precipitation from streamflow observations in basins of the Sierra Nevada mountain range of California. This region features large, topographically-driven gradients of precipitation, and it is a critical water supply region for the state. In addition, there is substantial uncertainty regarding precipitation falling in high-altitude basins, which impacts the ability of downstream operators to function efficiently. The southern portion of the range is also known to be a location of errors in gridded "reference" precipitation products (Mote et al., 2005), presumably due to a lack of high-elevation precipitation gauges. It also is the location of observed year-to-year changes in the spatial pattern of precipitation and snowpack (Aguado, 1990), which highlight the need for precipitation estimates that do not rely on climatological spatial patterns.

The precipitation in this region is predominantly snow, due to its Mediterranean climate and high altitude, and thus, the application of precipitation inference from streamflow requires simulation of snowpack. Snowpack simulation in the "doing hydrology backward" framework is novel, and challenges our ability to identify precipitation, because the basin's response to many precipitation input events is aggregated into melting of the snowpack in spring and summer. As a result, it was necessary to construct a new temperature-index snow model coupled with an existing hydrologic model for this study (see methods section). Additionally, we estimate precipitation at the annual timescale or longer, because of the snow-dominated, wet winter/dry summer climate of these watersheds. This avoided the need to disaggregate runoff events into individual storm events.

Earlier studies using streamflow measurements at multiple sites to infer precipitation patterns have shown promise in the Sierra Nevada (Lundquist et al., 2009, 2003). We hypothesize that this approach could generate an improved understanding spatially-distributed precipitation patterns by considering multiple high-altitude basins within a single region. We test whether or not the inferred precipitation patterns appear consistent with other spatial estimates of precipitation based on climatology. We also investigate the sensitivity and uncertainty of the precipitation-from-streamflow approach, and evaluate the usefulness of this approach in comparison with currently-employed techniques.

The methods section describes the conceptual approach, the hydrologic model (FUSE) and the calibration routine (BATEA) used to infer basin-mean precipitation. The data section lists the hydrological, topographical and meteorological data used in this study. In the results, we present the inferred basin-average precipitation in our test basins, both the long-term mean and examples of year-to-year variability. In the discussion section, we evaluate the precision of this method and its sensitivity to the assumptions made in this study. The conclusion discusses the potential of this method for improving understanding of mountain precipitation and outlines further work.

METHODS: PRECIPITATION INFERENCE

Conceptual Approach

We seek to infer basin-mean precipitation, over timescales of a year or longer, given observed streamflow records for the basin. This is an application of Bayes' Theorem in which, for a given time period, the probability distribution function of the basin-mean precipitation multiplier M, given observed streamflow $\tilde{Q}$, is

$$\boldsymbol{P}\left(M|\tilde{Q}\right) = \frac{\boldsymbol{P}(\tilde{Q}|M)\cdot\boldsymbol{P}(M)}{\boldsymbol{P}(\tilde{Q})} \quad [2].$$

Thus, we estimate the probability distribution function (PDF) of the multiplier M that relates the gauge precipitation to the true basin-mean precipitation. The first term in the numerator of (2) is the likelihood function, which describes the basin's odds of generating the observed streamflow $\tilde{Q}$ given the observed precipitation gauge record and some value of M. Estimation of this function requires an understanding of the basin's hydrologic response, and this is the role of the hydrologic model that we describe below. The second term in the numerator of (2) is the a priori distribution of the precipitation multiplier; the expectation that the gauge precipitation underestimates the basin-mean precipitation is reflected in a mean multiplier of less than one. The posterior distribution of the precipitation given streamflow, $\boldsymbol{P}\left(M|\tilde{Q}\right)$, represents the updated distribution of precipitation multiplier likelihood once streamflow information has been incorporated. In practice, we also estimate additional parameters related to the hydrologic model simultaneously with the precipitation multiplier. This includes the orographic precipitation gradient (OPG), which is used to distribute precipitation among the elevation bands of the snow model (see below). Once the PDFs of the multiplier and the OPG are inferred, they can be used along with the gauge record to calculate the PDF of the basin-mean precipitation.

Figure 1 shows a schematic of information flow in the precipitation inference routine. Forcing data and prior parameter distributions (described in the data section) are used to simulate an ensemble of basin simulations using different parameter sets. The snow and soil models (described in this section below) simulate both SWE and soil moisture, which are then used to generate modeled runoff time series. The ensemble of runoff time series is compared with the observed streamflow record using BATEA (also described below), and the updated parameter distributions result. From the posterior distributions of the rainfall multiplier, the optimal basin-mean precipitation is then calculated along with its confidence limits from the ensemble of samples. This allows us both to estimate basin-mean precipitation from streamflow and to ascertain the uncertainty of the inferred precipitation rate.

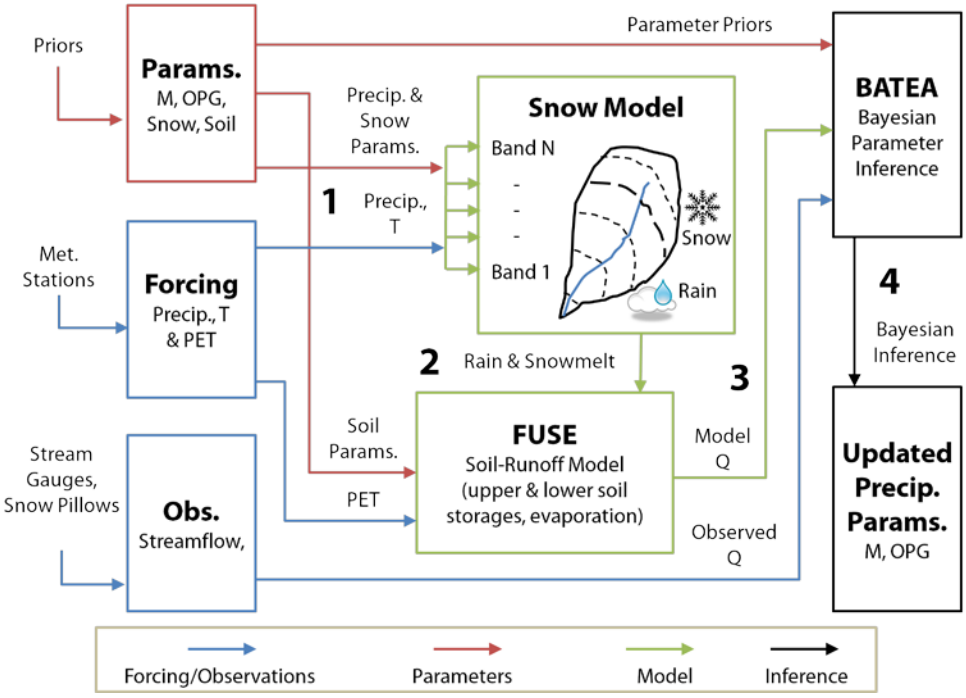

Figure 1. Schematic of information flow in the FUSE-snow model-BATEA calibration routine. Forcing data from meteorological stations are combined (1) with parameters such as the rainfall multiplier (M) the orographic precipitation gradient (OPG), and soil and snow parameters, to simulate basin snowpack (2) and runoff (3). The simulated runoff is then compared with observed values, using a Bayesian approach that incorporates prior information in BATEA (4). The result is a posterior distribution of parameters, including M and OPG, which describe the basin-mean precipitation probability distribution

FUSE Conceptual Rainfall-Runoff Model

In order to calculate $\boldsymbol{P}(\tilde{Q}|\mathrm{M})$ in (2), we use a conceptual rainfall runoff model, the Framework for Understanding Structural Uncertainty (FUSE) model (Clark et al., 2008). FUSE is a lumped model which represents soil moisture storage and fluxes such as evapotranspiration, surface runoff and baseflow. The model represents basin runoff response via upper, unsaturated and lower, saturated soil zones. As a relatively simplified, lumped model, FUSE has fewer tunable parameters than many other hydrologic models, which simplifies the calibration process. The FUSE model has been incorporated into BATEA, allowing the modeler to simulate multiple model structures within the precipitation input uncertainty and Bayesian calibration environment.

Basin Snow Model

Because FUSE did not simulate snow, and the hydrology of the basins in question is snow-dominated, we built a temperature index snow model which is coupled to FUSE. The snow model is based on Snow-17 (Anderson, 2006), in which snow water equivalent (SWE) is tracked based on precipitation and melt. Precipitation adds to SWE if the air temperature is below a threshold, and generates soil input water otherwise. Melt is initiated if the air temperature is above another threshold, and is proportional to temperature over that threshold. Snowmelt is immediately provided to the soil model.

In order to simulate the strong elevation dependence found within the Sierra Nevada basins, the snow model is run at 100m elevation bands, unlike the lumped soil model. Elevation bands can provide a method of simulating the within-basin snowpack variability that is necessary to generate accurate streamflow recession (Clark et al. 2011). For each band, temperature from the forcing dataset is lapsed to *i*th band midpoint elevation using the following relation:

$$T(i) = T_f + \Gamma(\mathrm{z_i} - \mathrm{z_f}) \quad [3]$$

where $T(i)$ is the *i*th band temperature, T_f is the forcing temperature, $\mathrm{z_i}$ is the band midpoint elevation, $\mathrm{z_f}$ is the forcing sites' average elevation, and Γ is temperature lapse rate (<0, °C km^{-1}). Γ is a parameter that is inferred in the calibration process. Similarly, precipitation is distributed to each band via a multiplicative scaling of the forcing precipitation:

$$P(i) = MP_f\,(1 + \alpha[\mathrm{z_i} - \mathrm{z_f}]) \quad [4]$$

where $P(i)$ is the ith band precipitation, P_f is the forcing precipitation, m is the gauge-to-basin precipitation multiplier, and α is the orographic precipitation gradient (OPG) in km^{-1} (Lundquist et al., 2010). The negative lapse rate and the positive OPG ensure that the higher bands are colder and have more precipitation, thus allowing the model to simulate high-elevation snowpack lasting into the summer.

Finally, water fluxes to the into the lumped soil model are calculated by a weighted average of rain plus snowmelt from each elevation band:

$$F_{soil} = \sum_{i=1}^{n_{bands}} AF_i(R_i + SM_i) \quad [5]$$

where F_{soil} is the flux of water into the soil, and AF_i is the fraction of the basin area, R_i is rain, and SM_i is the snowmelt, all from band i.

BATEA Calibration Routine

The calibration of the FUSE model proceeds in BATEA following the conceptual framework of Bayes' Theorem described by (2). BATEA compiles prior information about the soil and snow model parameters, as well as the precipitation multiplier and OPG, and then simulates basin runoff using a variety of parameter sets. The simulated runoff is compared to the observed streamflow, and those parameter sets which produce both smaller streamflow errors and have higher prior parameter likelihood result in the highest posterior parameter likelihood. To sample the posterior probability distributions for a parameter space with high dimensionality (the combination of the soil, snow meteorology and error model parameters results in at minimum a 16-dimensional parameter space), a Monte Carlo Markov Chain (MCMC) algorithm is implemented in BATEA (Kavetski et al., 2006). The result of the

MCMC routine is a distribution of parameter-space samples, with more samples clustered around parameter values with greater posterior likelihood.

The capacity of the model calibration scheme to identify the "true" precipitation is limited by the amount of information contained in the streamflow time series. For example, the correction factor on the gauge precipitation may not be identifiable if it is compensated for by other model parameters which are similarly uncertain. This problem of identifiability may limit the extent of parameter inference, but can be reduced if useful prior information is known and can be applied to the other parts in the model (Renard et al., 2010). In the case of mountain basins, this requires at least some knowledge of the soil characteristics and snow model parameters, as well as the temperature and potential evapotranspiration forcing data. The information used to generate the prior distributions is discussed in the next section.

We used the BATEA calibration routine with a weighted least squares (WLS) error model. The error model is used by the BATEA MCMC routine to translate errors in modeled and observed streamflow into the likelihood of a given parameter set. WLS refers to preferentially weighting errors at different timesteps, depending on the modeled streamflow, as opposed to standard least squares weighting, which treats all errors equally. Specifically, we hypothesized that due to uncertainties in the inputs, the model processes, and the measured streamflow, the absolute streamflow error can be expected to increase at higher flow rates. Employing WLS error models has been shown to improve the robustness of the model calibration by avoiding overfitting to large, potentially anomalous flood events (Thyer et al., 2009).

Inferring Long-Term Basin-Mean Precipitation vs. Individual Years

Initially, we infer long-term basin-mean precipitation rates over the study period of the 1981-2006 water years. For these studies, the soil, snow and precipitation parameters are all allowed to vary during the calibration process, and the parameter prior distributions described below is applied. Using a long calibration period should avoid calibration errors associated with anomalous water years. The inferred soil and snow model parameters, derived from the long-term calibration, can then be used as fixed quantities in subsequent shorter-term studies. In these cases, we assume that the soil and snow model parameters are essentially constant, but that precipitation multiplier, the OPG and the temperature lapse rate may vary substantially at the year-to-year timescale. For individual years, in this study 2005 and 2006, we repeat the calibration only allowing those three parameters to vary, with all other parameters fixed at their 1981-2006 calibration optimal values.

DATA

In order to operate the calibration and precipitation inference routine described above and depicted in Fig. 1, the following data are required: basin elevation distributions, daily streamflow observations, daily precipitation, temperature and potential evapotranspiration forcing data, and information about the probability distributions of soil parameters, snow model parameters, and the precipitation multiplier, OPG and temperature lapse rate.

Yosemite-Area Basin Data

Our study area includes sub-basins of the Tuolumne and Merced Rivers on the west slope of the Sierra Nevada mountain range of California (Figure 2). The basins include the Tuolumne River above Hetch Hetchy Reservoir, the Merced River above both Happy Isles and Pohono Bridge, and the basins above Cherry Lake and Lake Eleanor. All of the basins are in or adjacent to the boundaries of Yosemite National Park, with the Merced and Tuolumne basins composing the majority of the park's high country wilderness area. The basins feature a mix of coniferous forests, meadows and high alpine open areas. Summers are warm and dry, while winters are cool with most precipitation falling as snow at the higher elevations, and as a mix of rain and snow at the lower elevations. The Tuolumne, Cherry, and Eleanor basins drain to reservoirs which are operated for water supply and hydroelectric generation. Topographical boundaries of the basins were delineated based on 30 m USGS topographical data, which were also used to calculate basin area-elevation distributions in 100 m elevation bands. The basins' elevations range from approximately 1000-4000 m.a.s.l. Information about the basin areas and elevation distributions is shown in Table 1.

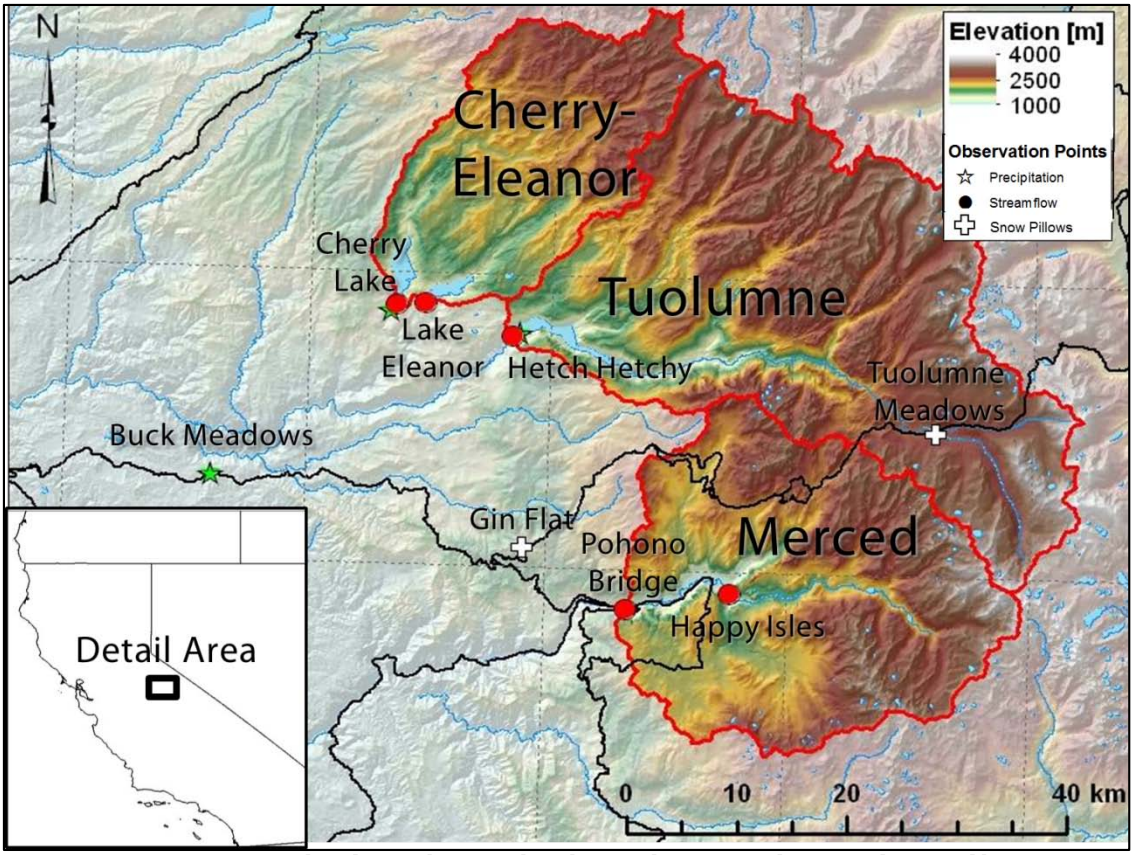

Figure 2. Yosemite area topographical map showing the Cherry-Eleanor, Tuolumne and Merced basins. Stream gauges are shown with red circles and meteorological stations are shown with stars. The lower Merced basin is the Pohono Bridge, and the upper basin is Happy Isles.

Table 1. Descriptions of the four study basins' areas, elevation ranges and mean streamflows.

Basin Name	Area [km^2]	Area Elevation Distribution Percentiles [m]			No. 100m Bands	Mean Streamflow [mm/d]
		10th	50th	90th		
Merced R. at Pohono Bridge	834	2097	2548	3142	29	2.05
Merced R. at Happy Isles	470	2184	2779	3265	28	2.03
Cherry Lake/ Lake Eleanor	492	1681	2310	2801	20	3.44
Tuolumne R. at Hetch Hetchy	1181	1998	2789	3238	30	2.36

Streamflow Observations

Daily streamflow observations from USGS stream gauges at Happy Isles and Pohono Bridge on the Merced River in Yosemite Valley were obtained. These gauges provide a long-term record of unimpaired runoff from the alpine Upper Merced basin. The Happy Isles basin is nested within the Pohono Bridge basin. Uncertainties in the streamflow measurements from the rating curve have been estimated at 10% or less (Rockwell, 1997).

Additionally, reconstructed full natural flows from the reservoir operators at Hetch Hetchy Reservoir and Cherry and Eleanor Lakes were provided by Hetch Hetchy Water and Power. The full natural flows estimate the discharge in the absence of the dams, based on observed reservoir releases and water levels. The uncertainties

associated with reconstructed flows are less well known. Because the adjacent Cherry and Eleanor Lakes are connected via a pumping tunnel with uncertain discharge, we summed their watershed areas and discharge time series to create a combined basin, herein referred to as Cherry-Eleanor.

Precipitation Observations

While the goal of this study is to infer basin-average precipitation, a time series of observed precipitation is still required in order to provide timing of basin water input. Precipitation observations were made at three low-elevation gauges (Hetch Hetchy, Cherry Lake and Buck Meadows, Figure 2). The gauges' mean annual precipitation during the study period are 960, 1303 and 935mm, respectively, and their elevations are 1180, 1453 and 976 m.a.s.l., respectively. The gauges are manually maintained during the winter and are at elevations where snow is less likely to cause significant measurement bias; no reliable high-elevation precipitation gauge records were available in the study area. We use an average of the three gauges' daily precipitation as the forcing series for the hydrologic model. Because the mean precipitations of the three gauges are fairly similar, biases due to small periods of missing data at any one particular gauge are not likely to be large.

Temperature Observations

Daily high and low temperatures were also available from the three precipitation sites. We averaged the high and low temperatures at each site to create a daily mean temperature, and then averaged the three stations' mean temperatures, to create one forcing time series of daily mean temperature.

Potential Evapotranspiration Estimates

A forcing time series of potential evapotranspiration (PET) is necessary for hydrologic modeling, and several approaches were developed to estimate basin-average PET. Pan evaporation measurements were made at Hetch Hetchy during summers from 1955-1978, and a regression was developed to relate PET to daily high and low temperatures and precipitation at the site. This regression was used to extend the PET estimate to the entire study period. In order to reflect the likely decrease in PET with elevation, the regression model was run at each 100m elevation band within a basin, using a -6.5 °C/km lapse rate to adjust temperatures from the observation sites' elevation. The basin-averaged PET was then calculated as the weighted average of the bands' series, based on the relative fraction of the basin area within each band.

Soils Information

In order to provide informative prior distributions for the calibration of the basin hydrologic models, information was collected on the typical basin soil properties. Being near the crest of the Sierra Nevada, the majority of the basins have steep topography that is underlain by granitic bedrock. Typical soils are shallow and sandy, with a depth of no more than 1 m and a porosity of about 0.4 (NRCS, 2006). Field studies have indicated that the soil has a high conductivity typical of sand and gravel, but that the percolation rate into the underlying bedrock is much less (Flint et al., 2008). A modeling study of the upper Merced basin indicated that the soils' conductivity was likely at least 1m day^{-1} and the field capacity was not likely more than 0.2-0.25, in order to match observed streamflow patterns (Lundquist and Loheide, 2011). In general, uniform distributions were used, and when no information was available about a parameter for the Yosemite domain, the distribution was set to the default limits for the FUSE model (Clark et al., 2008).

PRISM Precipitation Data

In order to obtain another estimate of basin-wide precipitation in the region, we used the PRISM climatological precipitation product (Daly et al., 2008). This is based on precipitation records from 1981-2010, and is provided at an 800 m resolution over the domain. For each basin, all PRISM cells within the watershed were used to find the average annual precipitation. The nearest PRISM cell to each of the three precipitation gauges were also averaged, and the PRISM ratio of basin to gauge precipitation was calculated. The annual observed precipitation from the gauges was then scaled by this ratio for each basin, in order to provide a PRISM-based estimate of the basin-mean precipitation.

RESULTS: BASIN-MEAN PRECIPITATION INFERRED FROM STREAMFLOW

Climatological (1981-2006) Precipitation

The results of precipitation inference for all four basins and for the entire study period (water years 1981-2006) are shown in Fig. 3. In the upper panel, histograms of the inferred basin-mean precipitation from the MCMC

sampling routine, which generated 4000 samples, are plotted. The Tuolumne and the Merced at Pohono and at Happy Isles basins have relatively similar precipitation rates, with overlap between the histograms of each. However, Cherry-Eleanor Lakes' basin is inferred to be significantly wetter, with a mean precipitation rate of approximately 1900 mm/yr. Additionally, the uncertainty of the precipitation estimates, as indicated by the width of the sample histograms, is approximately +/- 50 mm/yr for each basin.

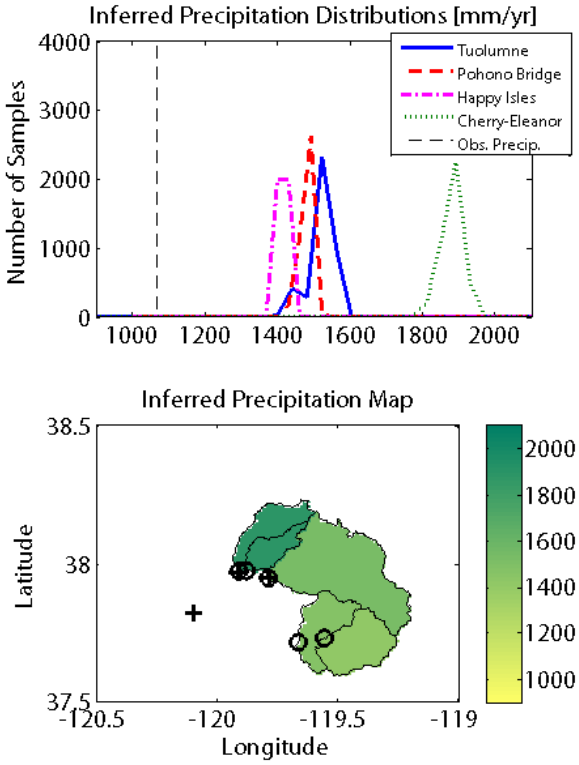

Figure 3. Climatological (1981-2006) inferred precipitation by basin. The sample distributions of the basin-mean precipitation from the MCMC inference routine are shown in the top panel. In the bottom panel, the mean of the distributions are plotted spatially. Stream gauges are shown with circles, and precipitation and temperature stations are shown with crosses.

In the lower panel of Figure 3, a spatial map of precipitation inferred for each basin is shown. The within-basin precipitation variability is not inferred in this experiment, and so each basin is shown as having uniform spatial precipitation rates. However, using only basin-mean values, it is possible to see a north-south precipitation gradient, in which Cherry-Eleanor is the wettest basin, while the Merced basins are relatively drier, with the Tuolumne in between. Thus, inferring precipitation from streamflow suggests that mean annual precipitation rates increase from south to north in this domain.

To compare our inferred precipitation against other estimates of basin-mean precipitation, we plotted the inferred mean precipitation for each basin against those found from PRISM (Daly et al., 2008) and from a simple scaling of observed streamflow (Figure 4). In the left panel, streamflow-inferred precipitation is plotted against the PRISM derived basin-mean precipitation. In all basins, the inferred streamflow is greater than that derived from PRISM. The difference is especially large in the Cherry-Eleanor basin, in which streamflow-derived precipitation is nearly 500 mm/yr greater than PRISM.

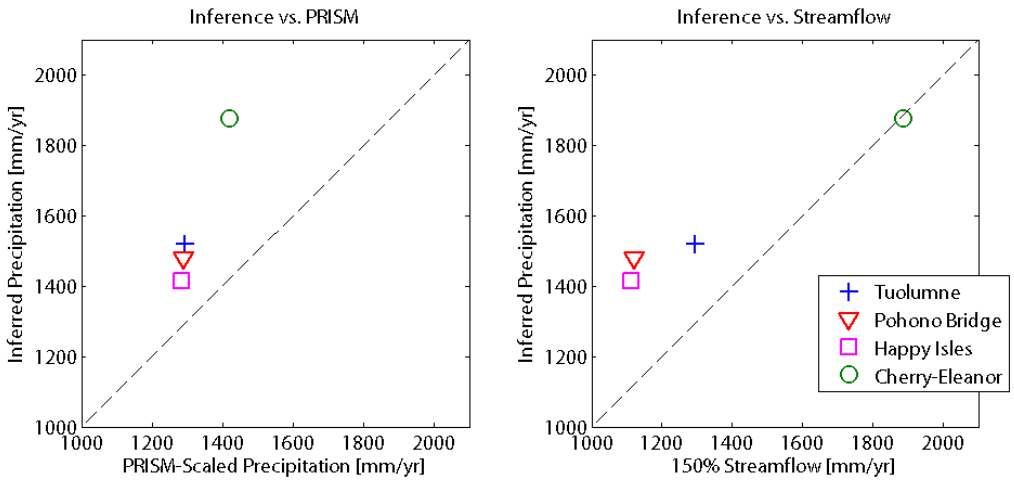

Figure 4. Comparison of inferred climatological precipitation to other estimates of basin-averaged precipitation. The left panel compares inferred precipitation (y-axis) and PRISM (x-axis). The right panel compares inferred precipitation with precipitation calculated by assuming an evaporation ratio of one-third.

We also plot inferred precipitation from the BATEA and FUSE routine against a simpler scaling of observed streamflow (Figure 4, right panel). Based on prior studies of Yosemite-area evapotranspiration, a runoff ratio of 0.65-0.7 has been suggested (Lundquist and Loheide, 2011). Thus, a simple method of obtaining precipitation from streamflow would be to multiply observed streamflow by 150%. The results indicate that the two methods agree fairly well, especially for the Cherry-Eleanor basin. However, the points above the 1:1 line (Tuolumne, Pohono Bridge and Happy Isles) suggest that the runoff ratio for these basins, as obtained by calibration of the FUSE model, is less than two-thirds.

Inference of 2005-2006 Precipitation Anomalies

Over the Yosemite region, divergent spatial patterns of precipitation were observed between water years 2005 and 2006. This is illustrated by the relative SWE at two snow pillows, Gin Flat near the Merced watersheds, and Tuolumne Meadows in the upper Tuolumne basin. In 2005, Gin Flat had relatively greater peak SWE, while in 2006, the relative rank was reversed (Figure 5, upper panels). The relative patterns in 2005 and 2006 are also reflected in the observed streamflow of the Tuolumne River and the Merced River at Pohono Bridge. The Tuolumne and the Merced had very similar runoff totals per unit basin area in 2005, but in 2006 the Tuolumne had approximately 15% more total runoff per unit area (Figure 5, middle panels). This suggests that the spatial patterns of precipitation differed between the two years, with a relatively greater shift to the south in 2005 compared to 2006.

To test this, we inferred basin-mean precipitation for these two basins only based on water year 2005 streamflow observations, and then repeated the analysis using only water year 2006 for calibration. As described in the methods section, these individual year calibrations only inferred the precipitation multiplier, OPG and temperature lapse rate, while leaving all other soil and snow model parameters fixed at their optimal values from the previous 1981-2006 calibration. The results are shown in the bottom panels of Figure 5. In 2005, it is inferred that the Merced at Pohono Bridge had approximately 1280 mm of precipitation, while the Tuolumne at Hetch Hetchy had just less than 1200 mm. In 2006, both basins received more precipitation, but it is inferred that the Tuolumne had nearly 1500 mm, or almost 40 mm more than the Merced at Pohono Bridge. The reversal of the order of the precipitation between the two basins over these two years is consistent with the observations of snowpack and streamflow. Thus, the method of inferring precipitation from streamflow appears capable of detecting year-to-year shifts in spatial precipitation patterns.

DISCUSSION: METHOD SENSITIVITY AND UNCERTAINTY

The spread of the histograms in Figure 3 indicate that the uncertainty associated with inferring the basin-mean annual precipitation rate from streamflow is approximately +/- 30-50 mm/yr. In a region with typical precipitation

rates of 1200-1800 mm/yr, this represents errors of +/- 2-4%, which is quite good compared other approaches of estimating basin-mean precipitation.

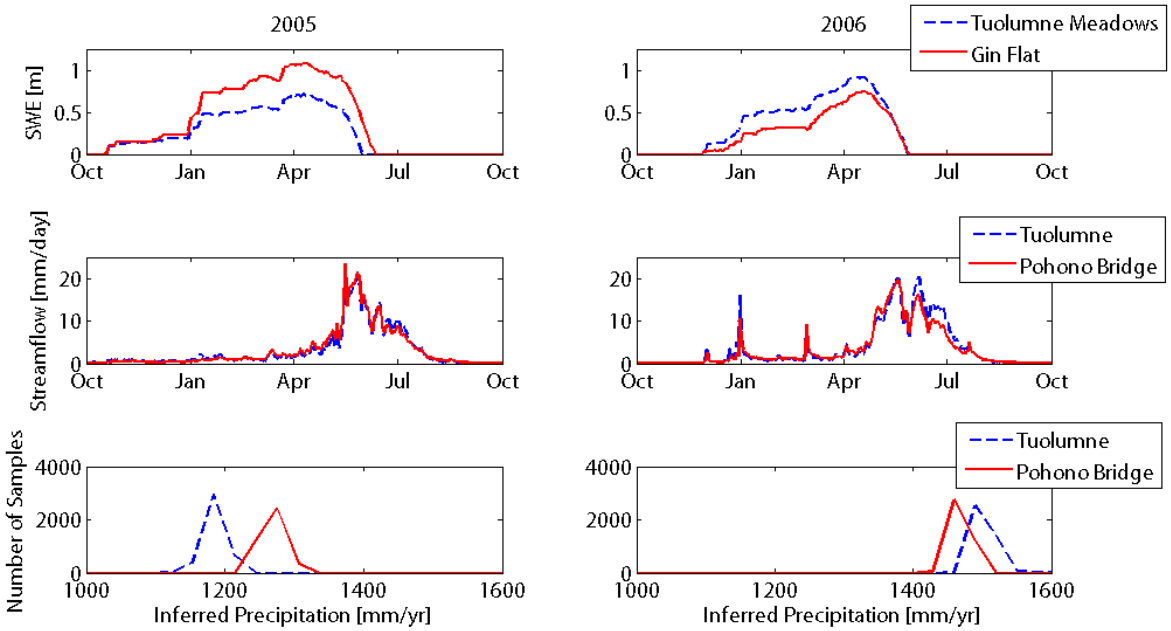

Figure 5. 2005 (left) vs. 2006 (right) comparison in the Tuolumne and Merced basins. Observed snowpack is shown in the top row at Gin Flat and Tuolumne Meadows. Observed streamflow in the Tuolumne and Merced at Pohono Bridge are shown in the middle row. The inferred precipitations for the river basins are shown in the bottom row.

However, it is important to test this method's sensitivity to the various model assumptions, forcing data, and parameter prior information that are used to drive the calibration process. By examining the sensitivity of the results, we can obtain an understanding of how precisely we may be able to estimate precipitation in mountain basins using streamflow. In particular, it is noted that the choice of PET forcing data is important to the ultimate result. Studies using alternative PET forcing series, derived either from the Penman-Monteith approach or from pan evaporation observations that are not scaled by elevation, show that the inferred precipitation rates change when PET forcing series of different magnitudes are used (not shown). This is due to the fact that the calibration seeks to close the basin water balance, so that a higher PET forcing results in more inferred precipitation. As a result, it is important to select PET data and methods that produce representative results for the basin and time period in question.

We are currently investigating method sensitivities such as this, as well as the influence of the choice of model structure and the soil parameter prior distributions. In order for this method to be applied robustly, the uncertainties associated with these choices must be explicitly identified. For example, the FUSE model allows for evaluation of different model structural choices such as the upper and lower zone storages and the evapotranspiration and baseflow parameterizations. The resulting uncertainty may be significantly larger than the +/- 30-50 mm/yr reported in these initial studies, which is something we seek to examine in future work.

CONCLUSION

Using streamflow data, a rainfall-runoff model, forcing data observed from nearby meteorological stations, and information about the soil and snow model parameters for the region, we inferred long-term basin-mean precipitation rates for four high-elevation basins in or near Yosemite National Park. We were able to infer the spatial pattern of precipitation over the four basins, showing reasonable match to PRISM climatological patterns, though some deviations were identified. Additionally, we were able to identify known spatial variations in precipitation

patterns between water years 2005 and 2006, using only the streamflow records from adjacent basins. The results indicate that this method may be capable of identifying basin-mean precipitation with useful precision.

For future work, beyond the sensitivity studies discussed above, we plan to extend this approach to more water years and basins. Many stream gauge records are available for the southern Sierra Nevada, a region of very high-elevation basins stretching from Yosemite National Park to Mt. Whitney. Precipitation gauges are very sparse here, and so the stream gauges will allow us to create a substantially more robust spatial map of precipitation patterns at the annual scale. Each basin, in effect, can act as a very large precipitation gauge, providing retrospective information about precipitation falling the watershed. For weather forecasters and water resource managers, annual scale spatial deviations from precipitation climatology are currently difficult to identify. This problem is particularly important in the high-elevation basins of the western United States. Our approach could help identify storm patterns that lead to such deviations, and thus improve future forecasts.

REFERENCES

Adam, J., E. Clark, and D. Lettenmaier. 2006. Correction of global precipitation products for orographic effects. *J. Clim.*, **19**, 15–38, doi:http://dx.doi.org/10.1175/JCLI3604.1. http://journals.ametsoc.org/doi/abs/10.1175/JCLI3604.1 (Accessed 5/29/2012).

Aguado, E. 1990. Elevational and latitudinal patterns of snow accumulation departures from normal in the Sierra Nevada. *Theor. Appl. Climatol.*,. http://link.springer.com/article/10.1007/BF00866873 (Accessed May 28, 2013).

Anderson, E. 2006. Snow accumulation and ablation model–SNOW-17. *On-line Doc.*,. http://scholar.google.com/scholar?hl=en&btnG=Search&q=intitle:Snow+Accumulation+and+Ablation+Model+–+SNOW-17#0

Clark, M. P., A. G. Slater, D. E. Rupp, R. a. Woods, J. a. Vrugt, H. V. Gupta, T. Wagener, and L. E. Hay. 2008. Framework for Understanding Structural Errors (FUSE): A modular framework to diagnose differences between hydrological models. *Water Resour. Res.*, **44**, W00B02, doi:10.1029/2007WR006735. http://www.agu.org/pubs/crossref/2008/2007WR006735.shtml

Clark, M.P., J. Hendrikx, A.G. Slater, D. Kavetski, B. Anderson, N. Cullen, T. Kerr, E.O. Hreinsson, et al. 2011: Representing spatial variability of snow water equivalent in hydrologic and land-surface models: A review. *Water Resour. Res.*, **47**, doi:10.1029/2011WR010745. http://www.agu.org/pubs/crossref/2011/2011WR010745.shtml.

Daly, C., M. Halbleib, J. I. Smith, W. P. Gibson, M. K. Doggett, G. H. Taylor, J. Curtis, and P. P. Pasteris. 2008. Physiographically sensitive mapping of climatological temperature and precipitation across the conterminous United States. *Int. J. Climatol.*, **28**, 2031–2064, doi:10.1002/joc.1688. http://doi.wiley.com/10.1002/joc.1688 (Accessed March 15, 2012).

Flint, A. L., L. E. Flint, and M. D. Dettinger. 2008. Modeling Soil Moisture Processes and Recharge under a Melting Snowpack. *Vadose Zo. J.*, **7**, 350, doi:10.2136/vzj2006.0135. https://www.soils.org/publications/vzj/abstracts/7/1/350.

Jankov, I., J.-W. Bao, P. J. Neiman, P. J. Schultz, H. Yuan, and A. B. White. 2009. Evaluation and Comparison of Microphysical Algorithms in ARW-WRF Model Simulations of Atmospheric River Events Affecting the California Coast. *J. Hydrometeorol.*, **10**, 847–870, doi:10.1175/2009JHM1059.1. http://journals.ametsoc.org/doi/abs/10.1175/2009JHM1059.1.

Kavetski, D., G. Kuczera, and S. W. Franks. 2006. Bayesian analysis of input uncertainty in hydrological modeling: 1. Theory. *Water Resour. Res.*, **42**, 1–9, doi:10.1029/2005WR004368. http://www.agu.org/pubs/crossref/2006/2005WR004368.shtml.

Kirchner, J. W. 2009. Catchments as simple dynamical systems: Catchment characterization, rainfall-runoff modeling, and doing hydrology backward. *Water Resour. Res.*, **45**, 1–34, doi:10.1029/2008WR006912. http://www.agu.org/pubs/crossref/2009/2008WR006912.shtml (Accessed March 9, 2012).

Luce, C. H., J. T. Abatzoglou, and Z. a Holden. 2013. The Missing Mountain Water: Slower Westerlies Decrease Orographic Enhancement in the Pacific Northwest USA. *Science*, **1360**, doi:10.1126/science.1242335. http://www.ncbi.nlm.nih.gov/pubmed/24292627 (Accessed December 13, 2013).

Lundquist, J., D. Cayan, and M. Dettinger. 2003. Meteorology and hydrology in yosemite national park: A sensor network application. *Inf. Process. Sens. …*, 518–528. http://www.springerlink.com/index/8gcqv9dmbaj9km6v.pdf.

Lundquist, J., B. Huggett, H. Roop, and N. Low. 2009. Use of spatially distributed stream stage recorders to augment rain gages by identifying locations of thunderstorm precipitation and distinguishing rain from snow. *Water Resour. Res.*, **45**, 1–7, doi:10.1029/2008WR006995. http://www.agu.org/pubs/crossref/2009/2008WR006995.shtml (Accessed March 8, 2012).

Lundquist, J. D., and S. P. Loheide. 2011. How evaporative water losses vary between wet and dry water years as a function of elevation in the Sierra Nevada, California, and critical factors for modeling. *Water Resour. Res.*, **47**, 1–13, doi:10.1029/2010WR010050. http://www.agu.org/pubs/crossref/2011/2010WR010050.shtml (Accessed March 9, 2012).

true, J. R. Minder, P. J. Neiman, and E. Sukovich. 2010. Relationships between Barrier Jet Heights, Orographic Precipitation Gradients, and Streamflow in the Northern Sierra Nevada. *J. Hydrometeorol.*, **11**, 1141–1156, doi:10.1175/2010JHM1264.1. http://journals.ametsoc.org/doi/abs/10.1175/2010JHM1264.1 (Accessed March 8, 2012).

Milly, P. C. D., and K. A. Dunne. 2002. Macroscale water fluxes 1. Quantifying errors in the estimation of basin mean precipitation. *Water Resour. Res.*, **38**, 1–14, doi:10.1029/2001WR000759. http://www.agu.org/pubs/crossref/2002/2001WR000759.shtml (Accessed May 25, 2012).

Mizukami, N., and M. B. Smith. 2012. Analysis of inconsistencies in multi-year gridded quantitative precipitation estimate over complex terrain and its impact on hydrologic modeling. *J. Hydrol.*, **428-429**, 129–141, doi:10.1016/j.jhydrol.2012.01.030. http://linkinghub.elsevier.com/retrieve/pii/S002216941200073X (Accessed March 8, 2012).

Mote, P. W., A. F. Hamlet, M. P. Clark, and D. P. Lettenmaier. 2005. Declining Mountain Snowpack in Western North America*. *Bull. Am. Meteorol. Soc.*, **86**, 39–49, doi:10.1175/BAMS-86-1-39. http://journals.ametsoc.org/doi/abs/10.1175/BAMS-86-1-39 (Accessed March 5, 2012).

Natural Resources Conservation Service. 2006. Soil Survey Geographic (SSURGO) database for Yosemite National Park, California, ca790, U.S. Dep. of Agric., Washington, D. C. (Available at http :// SoilDataMart.nrcs.usda.gov.)

Rasmussen, R., and Coauthors. 2011. The NOAA/FAA/NCAR Winter Precipitation Test Bed: How Well Are We Measuring Snow? *Bull. Am. Meteorol. Soc.*, 111130083336008, doi:10.1175/BAMS-D-11-00052.1. http://journals.ametsoc.org/doi/abs/10.1175/BAMS-D-11-00052.1 (Accessed July 6, 2012).

Renard, B., D. Kavetski, G. Kuczera, M. Thyer, and S. W. Franks. 2010. Understanding predictive uncertainty in hydrologic modeling: The challenge of identifying input and structural errors. *Water Resour. Res.*, **46**, W05521, doi:10.1029/2009WR008328. http://www.agu.org/pubs/crossref/2010/2009WR008328.shtml (Accessed January 29, 2013).

Rockwell, G. L., S. W. Anderson, and P. D. Hayes. 1997. Water resources data, California, Water Year 1996, vol. 3, Southern central valley basins and the great basin from Walker R. to Truckee River. U.S. Geol. Surv. Water-Data Rep. CA–96–3, 479 pp.

Roe, G. H. 2005. Orographic Precipitation. *Annu. Rev. Earth Planet. Sci.*, **33**, 645–671, doi:10.1146/annurev.earth.33.092203.122541. http://www.annualreviews.org/doi/abs/10.1146/annurev.earth.33.092203.122541.

Sieck, L. C., S. J. Burges, and M. Steiner. 2007. Challenges in obtaining reliable measurements of point rainfall. *Water Resour. Res.*, **43**, doi:10.1029/2005WR004519. http://doi.wiley.com/10.1029/2005WR004519 (Accessed April 9, 2014).

Thyer, M., B. Renard, D. Kavetski, G. Kuczera, S. W. Franks, and S. Srikanthan. 2009. Critical evaluation of parameter consistency and predictive uncertainty in hydrological modeling: A case study using Bayesian total error analysis. *Water Resour. Res.*, **45**, W00B14, doi:10.1029/2008WR006825. http://www.agu.org/pubs/crossref/2009/2008WR006825.shtml.

Vrugt, J. a., C. J. F. ter Braak, M. P. Clark, J. M. Hyman, and B. a. Robinson. 2008. Treatment of input uncertainty in hydrologic modeling: Doing hydrology backward with Markov chain Monte Carlo simulation. *Water Resour. Res.*, **44**, 1–15, doi:10.1029/2007WR006720. http://www.agu.org/pubs/crossref/2008/2007WR006720.shtml (Accessed March 5, 2012).

Wayand, N. E., A. F. Hamlet, M. Hughes, S. I. Feld, and J. D. Lundquist. 2013. Intercomparison of Meteorological Forcing Data from Empirical and Mesoscale Model Sources in the North Fork American River Basin in Northern Sierra Nevada, California*. *J. Hydrometeorol.*, **14**, 677–699, doi:10.1175/JHM-D-12-0102.1. http://journals.ametsoc.org/doi/abs/10.1175/JHM-D-12-0102.1.